

One-pot synthesis of substituted 4*H*-chromenes by nickel ferrite nanoparticles as an efficient and magnetically reusable catalyst

Hamideh AHANKAR¹, Ali RAMAZANI^{1,*}, Katarzyna ŚLEPOKURA², Tadeusz LIS², Sang Woo JOO³

¹Department of Chemistry, University of Zanjan, Zanjan, Iran

²Faculty of Chemistry, University of Wrocław, Wrocław, Poland

³School of Mechanical Engineering, Yeungnam University, Gyeongsan, Republic of Korea

Received: 09.10.2017

Accepted/Published Online: 05.02.2018

Final Version: 01.06.2018

Abstract: Nickel ferrite magnetic nanoparticles (NiFe₂O₄ MNPs) were prepared via the autocombustion assisted sol-gel method. The efficient catalyst was investigated by FT-IR, XRD, ICP, SEM, and TEM techniques. A one-pot, three-component reaction is reported for the synthesis of substituted 4*H*-chromenes in the presence of NiFe₂O₄ MNPs as a reusable catalyst in a green solvent at 40 °C under clean, efficient, and mild conditions. Furthermore, selected products were characterized by FT-IR, ¹H NMR, and ¹³C NMR. The single-crystal X-ray analysis of product **4u** was also conclusively confirmed. Easy workup procedure, high purity of products via simple recrystallization, and environmentally benign conditions are the outstanding benefits of this method.

Key words: Nickel ferrite, magnetic nanoparticles, multicomponent reactions, 4*H*-chromenes, green methodology

1. Introduction

In recent decades, multicomponent reactions (MCRs) have been frequently used by synthetic chemists as an effective method to generate molecular diversity because of the high variability in reaction components and conditions. Moreover, these reactions have gained remarkable interest for chemists as an appropriate, atom-economical, and time-saving procedure for the synthesis of various compounds with interesting properties.^{1–3} In recent years, many trends have emerged for the application of types of nanoparticles due to their potential features in various fields of modern organic synthesis and especially in MCRs.^{4,5} These types of reactions in the presence of magnetic nanoparticles (MNPs) have many advantages such as high yield, short reaction times, low cost, selectivity, clean reaction profiles, and ecofriendly and environmentally benign conditions in comparison to the various strategies of the classical chemistry.^{6–8} MNPs, and especially different ferrite MNPs with interesting properties as recoverable and reusable catalysts, are widely used in a variety of MCRs. The separation of MNPs with external magnets is one of the most promising strategies in organic synthesis.^{9,10} Spinel-type bimetal oxides such as NiFe₂O₄ MNPs show great potential in the catalysis field, although they have so far been less investigated.^{11,12}

Benzopyran is a class of heterocyclic organic compounds called chromene according to IUPAC nomenclature. Some structural scaffolds such as chromane, 2*H*-chromene, and 4*H*-chromene contain a benzopyran

*Correspondence: aliramazani@znu.ac.ir

nucleus (Figure 1).¹³ Chromenes are an important class of compounds found in many pharmaceuticals and active natural products.

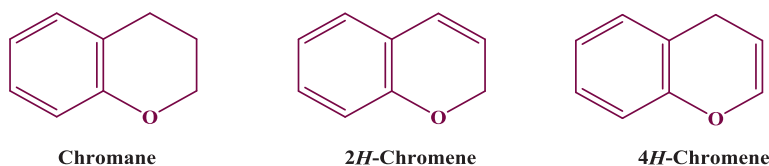


Figure 1. Different structural scaffolds containing a benzopyran nucleus.

Vitamin E (**1**) as a fat-soluble antioxidant¹⁴ and cromakalim (**2**), a potassium channel-opening vasodilator as an antihypertensive agent, are substances that include chromane moiety (Figure 2).¹⁵

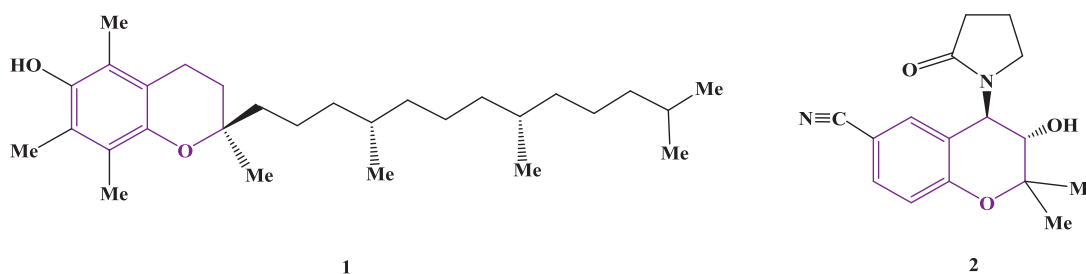


Figure 2. Selected drugs with chromane moiety.

Natural products with chromene moiety are rather unusual and only a few examples containing this structure have been isolated (Figure 3). Uvafzelin (**3**) was separated from the stems of *Uvaria afzelii* and presents a broad spectrum of antimicrobial activity versus gram-positive and acid-fast bacteria like *Mycobacterium tuberculosis*.¹⁶ Erysenegalensein C (**4**), isolated from the bark of *Erythrina senegalensis*, found potential use in the treatment of gonorrhoea, female infertility, and stomach pain.¹⁷ Meanwhile, 7-hydroxy-6-methoxy-4*H*-chromene (**5**) was obtained from the flowers of *Wisteria sinensis* and shows organoleptic features.¹⁸ Another natural compound, conrauinone A (**6**), was isolated from the bark of the tree *Millettia conraui* and used for the treatment of intestinal parasites.¹⁹

Substituted chromenes are known as interesting heterocyclic compounds with attractive biological and pharmacological activities including antioxidant,¹⁴ antitumor,²⁰ anti-HIV,²¹ antiinflammatory,²² antimicrobial and antifungal,²³ anticoagulant,²⁴ and diuretic activities.²⁵ Some drugs have chromene skeletons for the treatment of neurodegenerative diseases like Parkinson and Alzheimer disease or Down syndrome.²⁶ In addition, compounds with chromene moiety are often utilized in the fields of biodegradable agrochemicals, cosmetics, and pigments.^{13,27} Because of the significance of substituted chromenes, diverse synthetic methods have been reported,^{28–37} but there are fewer references about the use of MNPs for synthesis of these compounds.^{38–40}

Synthesis of heterocyclic compounds containing 4*H*-chromene skeletons has gained importance in organic synthesis because of their significant activities. Their various applications and high consumption, the small amounts of these compounds in natural resources, and, most importantly, the difficulty of their extraction have caused chemists to try synthesizing 4*H*-chromene derivatives. It should be noted that using various ferrite nanoparticles as green catalysts in MCRs is part of our ongoing program. In this study, we report a new method for the synthesis of substituted 4*H*-chromenes in the presence of nickel ferrite nanoparticles (NiFe₂O₄ MNPs) in a green solvent at 40 °C (Scheme 1).

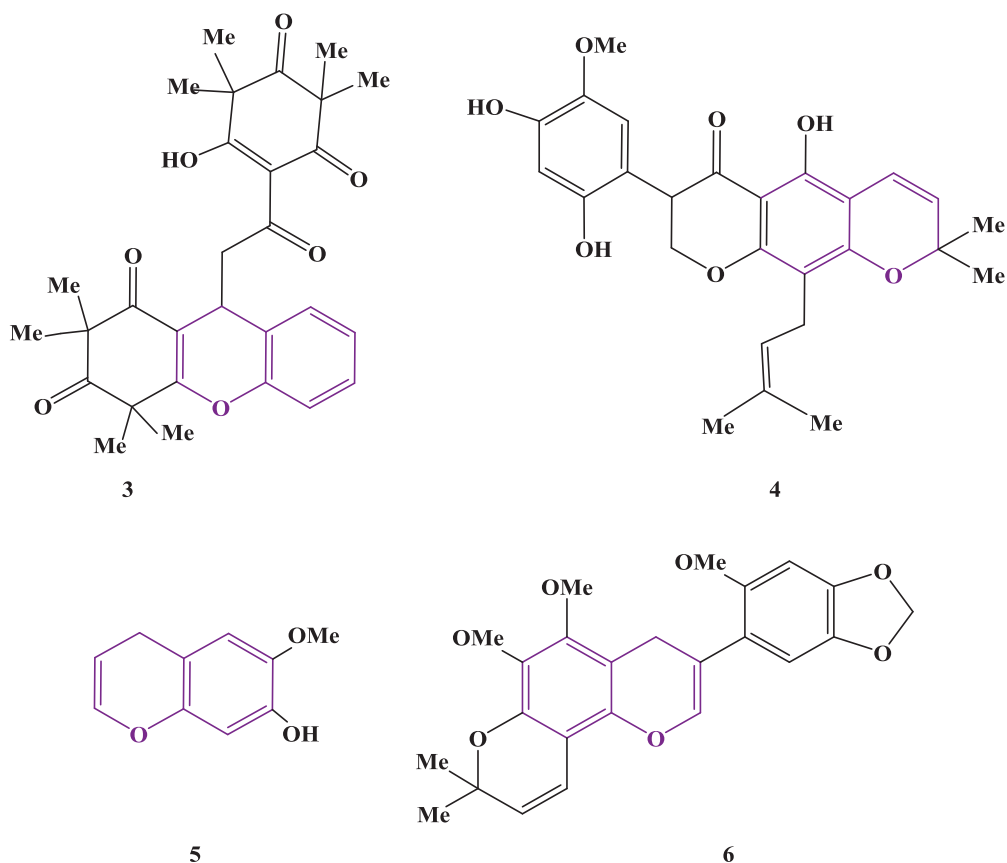
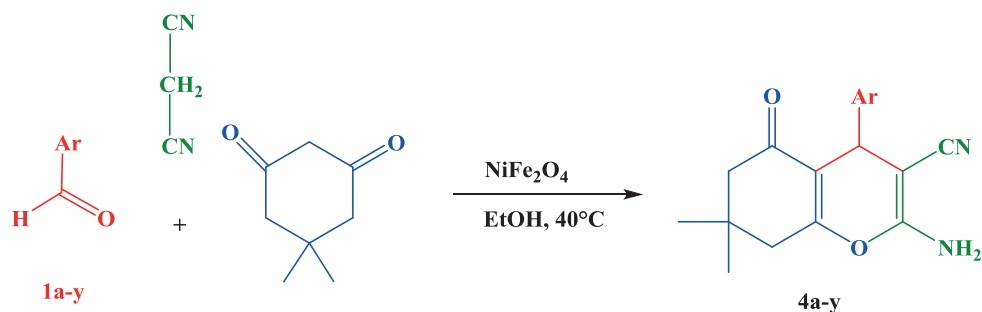


Figure 3. Selected natural products with chromene moiety.



Scheme 1. Synthesis of substituted 4*H*-chromenes.

2. Results and discussion

2.1. Characterization of catalyst

First, the structure of the NiFe_2O_4 MNPs was checked by Fourier transform infrared (FT-IR) spectroscopy. As shown in Figure 4, a broad absorption band above 3400 cm^{-1} is the stretching mode of H_2O molecules. Two principal absorption bands are observed in the range of $400\text{--}600\text{ cm}^{-1}$. Two absorption bands are observed at 587 and 458 cm^{-1} that demonstrate the longer and shorter bond length of oxygen metal ions in the octahedral and tetrahedral sites in the spinel structure, respectively. The atomic ratio of Ni/Fe was about 0.59, which is attributed to NiFe_2O_4 and 27.61% of its weight inclusive of nickel element according to ICP analysis.

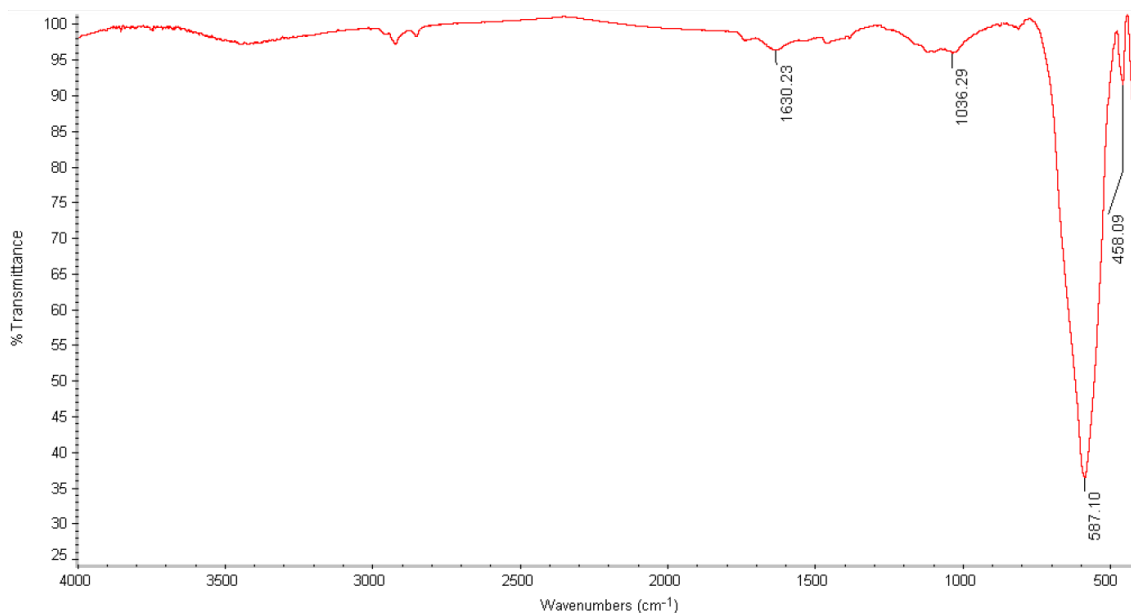


Figure 4. FT-IR spectrum of NiFe_2O_4 MNPs.

The strong diffraction peaks at the Bragg angles at 2θ of 30.45, 35.76, 37.30, 43.43, 53.84, 57.34, and 63.01 correspond to the (220), (311), (222), (400), (422), (511), and (440) facets of elemental nickel and iron, respectively, in X-ray diffraction (XRD) analysis (Figure 5). The average diameter was estimated to be about 59.7 nm by the Debye–Scherrer equation. It became clear that the structure of NiFe_2O_4 MNPs is a cubic spinel (JCPDS: 01-074-2081).

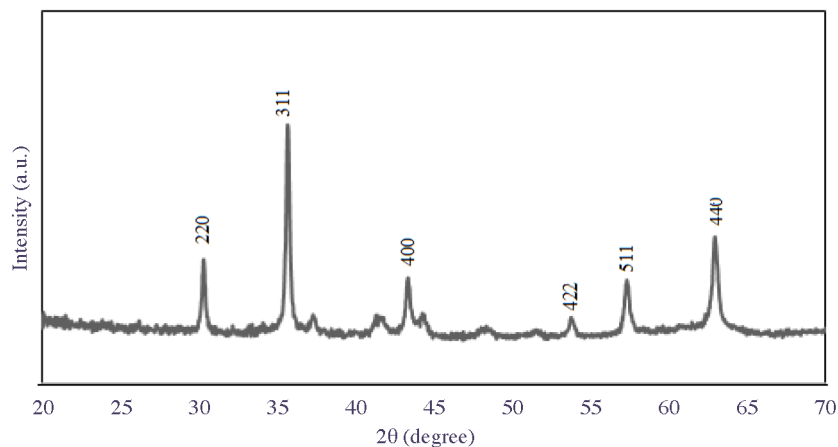


Figure 5. XRD pattern of NiFe_2O_4 MNPs.

In addition, the monotonous spherical morphology of the NiFe_2O_4 MNPs can be seen in the scanning electron microscopy (SEM) images. Measurements show that the mean size of the nanoparticles is 58.8 nm (Figure 6).

Furthermore, transmission electron microscopy (TEM) images show that NiFe_2O_4 MNPs have spherical morphology and the average particles size is 46 nm (Figure 7).

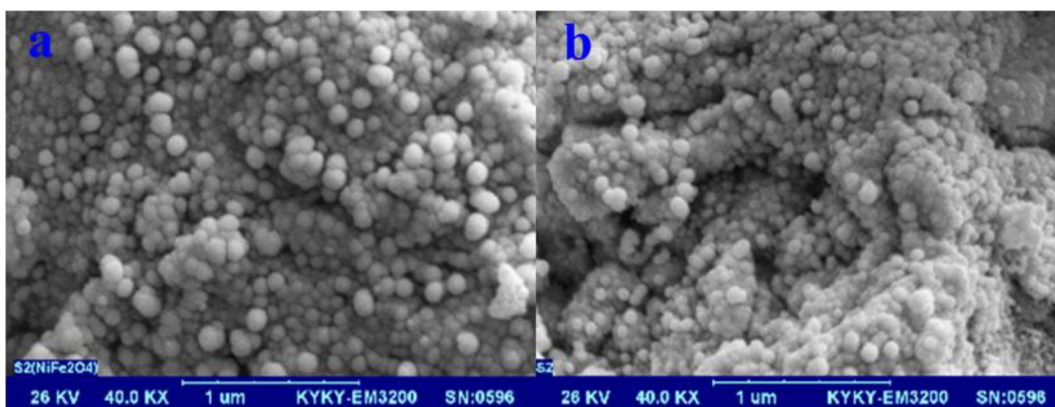


Figure 6. SEM images (a and b) of NiFe_2O_4 MNPs.

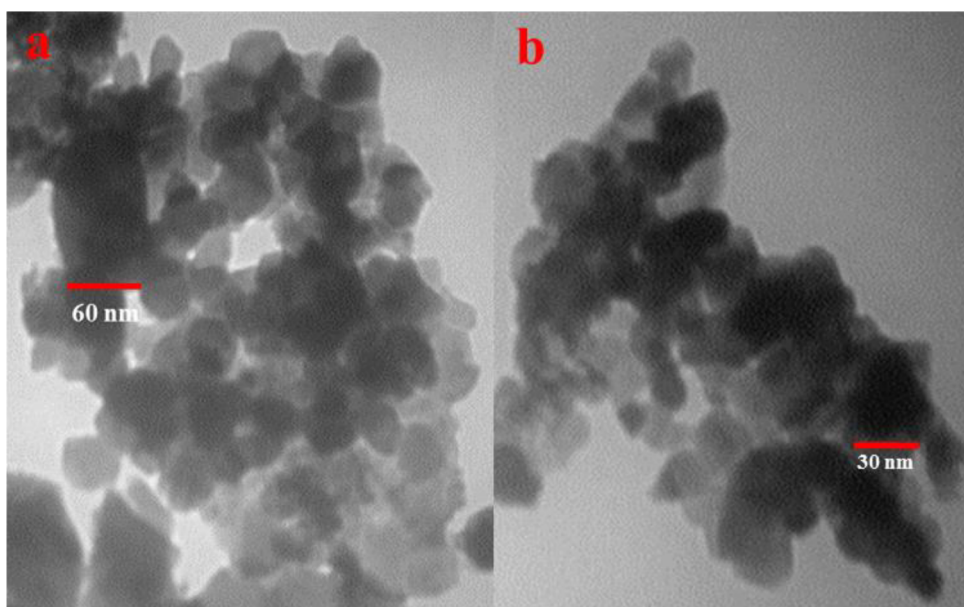


Figure 7. TEM images (a and b) of NiFe_2O_4 MNPs with magnification of $63,000\times$.

2.2. Application of NiFe_2O_4 MNPs in the synthesis of substituted 4*H*-chromenes

In order to find the optimal experimental conditions in this work, various conditions like reaction temperature, solvent, and catalyst were investigated in a convenient and easy method for synthesis of substituted 4*H*-chromenes. In primary research on the synthesis of compound **4a** from the reaction of 4-chlorobenzaldehyde, dimedone, and malononitrile in a suitable solvent by a magnetically reusable catalyst as a model reaction, it was found that the reaction did not proceed well at room temperature and a higher temperature was required. First, we optimized the effect of temperature through some experiments. To find the optimum temperature, synthesis of compound **4a** as a model of reaction was carried out at room temperature ($20\text{ }^\circ\text{C}$) and 30, 40, 50, and $60\text{ }^\circ\text{C}$ in ethanol solvent in the presence of NiFe_2O_4 MNPs (the results are shown in Table 1). The reaction yield was 48% after 60 min at room temperature (Table 1, entry 1), whereas yield of 95% was obtained at $40\text{ }^\circ\text{C}$ after 30 min (Table 1, entry 3).

Then, to find the best solvent, different solvents such as H_2O , $\text{H}_2\text{O}-\text{C}_2\text{H}_5\text{OH}$, $\text{C}_2\text{H}_5\text{OH}$, CH_3OH ,

Table 1. The effect of temperature on the synthesis of substituted 4*H*-chromenes.

Entry	Temperature (°C)	Time (min)	Yield (%) ^a
1	20 (r.t.)	60	48
2	30	30	62
3	40	30	95
4	50	30	95
5	60	30	97

Reaction conditions: 4-chlorobenzaldehyde **1a** (1 mmol), dimedone **2** (1 mmol), malononitrile **3** (1 mmol), and 11.7 mg of NiFe₂O₄ MNPs (5% mol) in ethanol and at various temperatures.

^a: Isolated yield.

CH₃CN, and CH₂Cl₂ were examined in the synthesis of **4a** as a model compound. The best result was obtained in ethanol, which occurred with 95% yield in 30 min at 40 °C (Table 2, entry 3). Other solvents were tested at the same time and temperature (Table 2, entries 1, 2, and 4–6), but the yield of the reaction was highest in ethanol. We thus selected ethanol as a green solvent for all our further reactions.

Table 2. The effect of the solvents on the synthesis of substituted 4*H*-chromenes.

Entry	Solvent	Temperature (°C)	Time (min)	Yield (%) ^a
1	H ₂ O	40	30	76
2	H ₂ O–C ₂ H ₅ OH	40	30	80
3	C ₂ H ₅ OH	40	30	95
4	CH ₃ OH	40	30	78
5	CH ₃ CN	40	30	75
6	CH ₂ Cl ₂	40	30	73

Reaction conditions: 4-chlorobenzaldehyde **1a** (1 mmol), dimedone **2** (1 mmol), malononitrile **3** (1 mmol), and 11.7 mg of NiFe₂O₄ MNPs (5% mol) in various solvents at 40 °C.

^a: Isolated yield.

Afterwards, the amount of the required catalyst was investigated in the model reaction mentioned above for synthesis of compound **4a**, as shown in Table 3 (entries 2–4). A yield of 38% for the desired reaction without catalyst was obtained after 30 min. No significant increase in yield was observed increasing the amount of catalyst by 2.5% mol. When 11.7 mg of NiFe₂O₄ MNPs (5% mol) was used, the maximum target product was produced.

After obtaining favorable results from the optimization of temperature, solvent, and catalyst amount, various aromatic aldehydes carrying electron-withdrawing and electron-donating groups on the aromatic ring in the *ortho*, *meta*, and *para* positions and heterocyclic, aliphatic, and unsaturated aldehydes were investigated. Yields of all the reactions were excellent. It was found that the aldehydes with electron-withdrawing groups reacted faster and better than the aldehydes with electron-donating groups (Table 4). The corresponding product **4** could not be generated when we used formaldehyde, glyoxal, acetaldehyde, isobutyraldehyde, salicylaldehyde, 5-bromosalicylaldehyde, and 2-hydroxy-1-naphthaldehyde under the reaction conditions, and in all cases,

Table 3. The effect of catalyst amount on the synthesis of substituted 4*H*-chromenes.

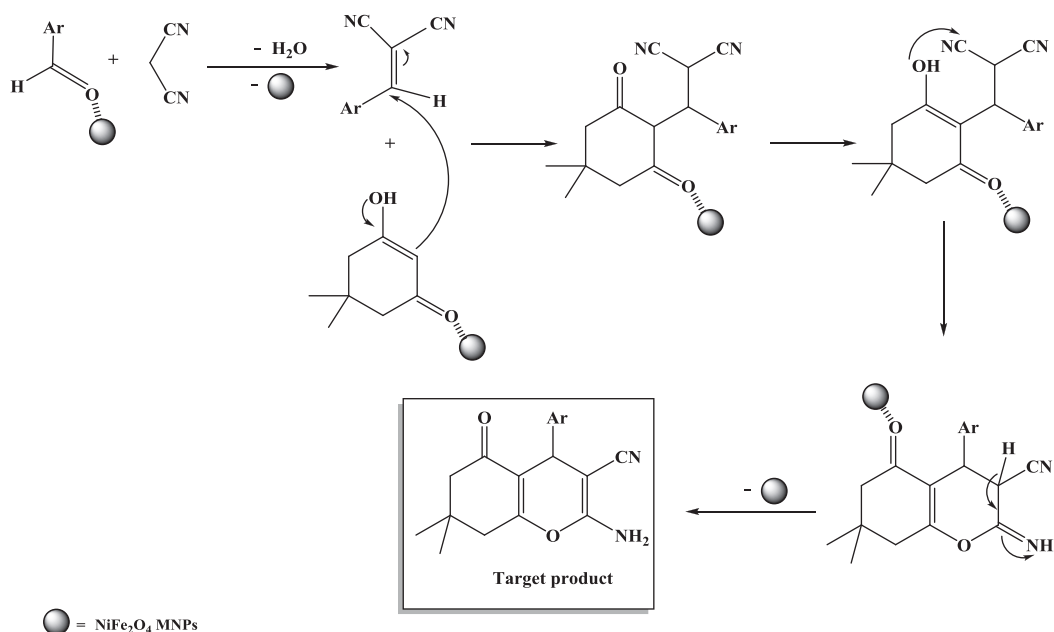
Entry	Catalyst (% mol)	Time (min)	Yield (%) ^a
1	None	30	38
2	2.5	30	66
3	5	30	95
4	7.5	30	93

Reaction conditions: 4-chlorobenzaldehyde **1a** (1 mmol), dimedone **2** (1 mmol), and malononitrile **3** (1 mmol), in ethanol solvent and various amounts of catalyst at 40 °C .

^a: Isolated yield.

a mixture of several products and starting materials was observed based on thin-layer chromatography (TLC) investigation.

The proposed mechanism for the synthesis of substituted 4*H*-chromenes is shown in Scheme 2. First a Knoevenagel reaction in the presence of NiFe₂O₄ MNPs, then Michael addition, and finally an intramolecular cyclization of the intermediate cause the target products.

**Scheme 2.** The proposed mechanism for the synthesis of substituted 4*H*-chromenes.

Ultimately, the reusability of the reaction catalyst was examined. After the magnetic separation of NiFe₂O₄ MNPs from the reaction mixture, the catalyst was rinsed with acetone and dried to eliminate any remaining acetone and reused again. NiFe₂O₄ MNPs were reused at least six times without serious reduction in their capability (Figure 8).

The structures of the selected products were confirmed by ¹H NMR, ¹³C NMR, and FT-IR spectroscopy. Melting points of products **4a–4y** were also measured. Finally, single-crystal X-ray analysis of **4u** conclusively confirmed its structure (Figure 9).

Table 4. Synthesis of substituted 4*H*-chromenes via a three-component reaction.

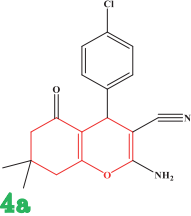
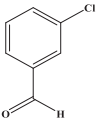
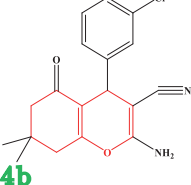
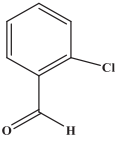
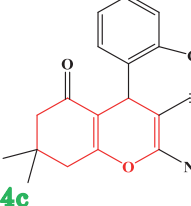
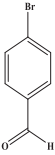
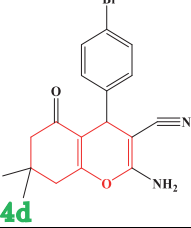
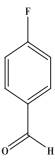
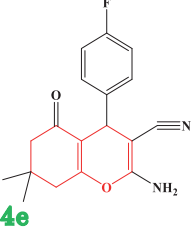
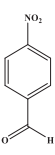
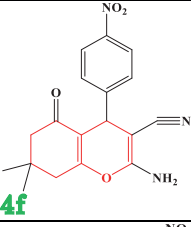
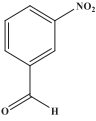
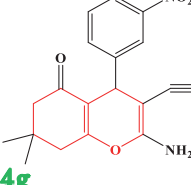
Entry	Aldehyde	Product	Time (min)	Yield (%) ^a	Mp (°C)	Mp ^{Ref} (°C)
1		 4a	30	95	214–216	215–216 ³²
2		 4b	35	92	237–239	235–237 ³³
3		 4c	30	91	215–218	214–215 ³⁴
4		 4d	40	88	214–217	205–207 ³⁰
5		 4e	30	86	209–211	210–211 ³²
6		 4f	25	90	181–183	180–182 ³⁴
7		 4g	40	88	213–215	214–216 ²⁹

Table 4. Continued.

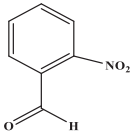
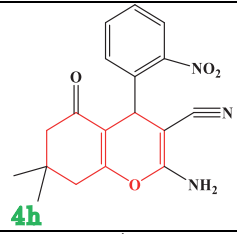
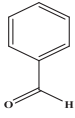
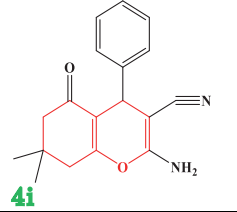
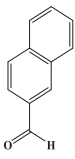
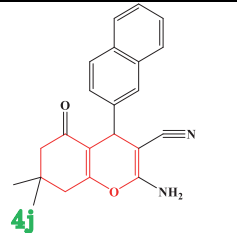
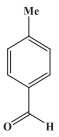
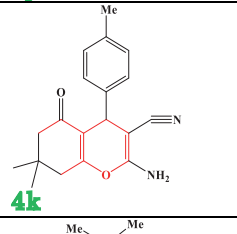
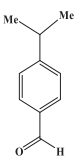
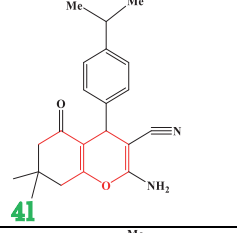
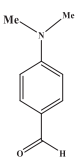
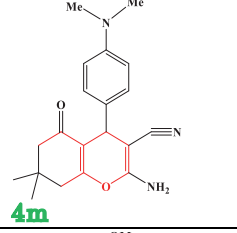
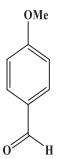
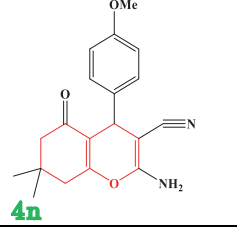
Entry	Aldehyde	Product	Time (min)	Yield (%) ^a	Mp (°C)	Mp ^{Ref} (°C)
8		 4b	25	85	231–233	233–234 ³²
9		 4i	35	90	235–237	234–235 ³²
10		 4j	30	92	248–252	230–232 ⁴⁰
11		 4k	50	87	210–212	214–215 ³³
12		 4l	50	89	206–208	204–206 ²⁹
13		 4m	45	90	216–218	217–218 ³²
14		 4n	60	91	201–203	201–202 ³²

Table 4. Continued.

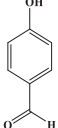
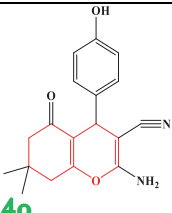
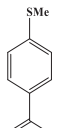
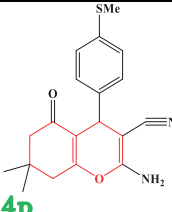
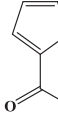
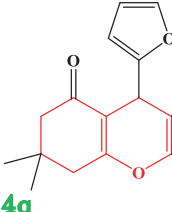
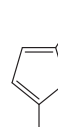
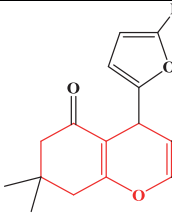
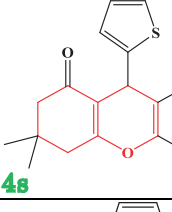
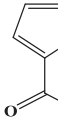
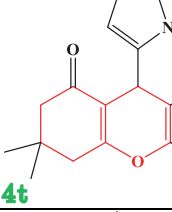
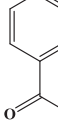
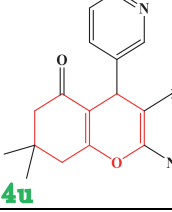
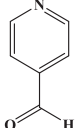
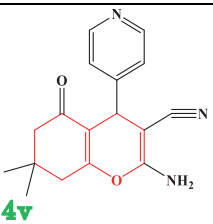
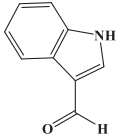
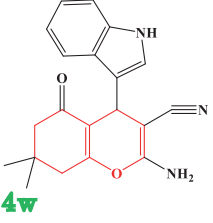
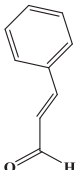
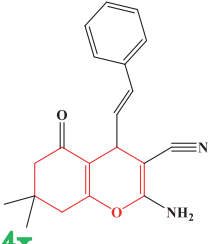
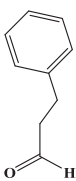
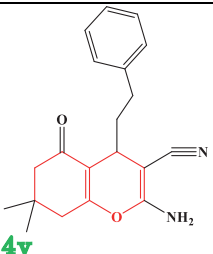
Entry	Aldehyde	Product	Time (min)	Yield (%) ^a	Mp (°C)	Mp ^{Ref} (°C)
15		 4o	60	87	225–227	222–224 ²⁹
16		 4p	60	90	239–242	211–212 ³⁵
17		 4q	45	89	224–226	226–228 ³²
18		 4r	35	83	180–182	
19		 4s	50	85	228–230	226–228 ³⁴
20		 4t	55	82	179–182	178–180 ³⁵
21		 4u	45	85	223–225	225–226 ³¹

Table 4. Continued.

Entry	Aldehyde	Product	Time (min)	Yield (%) ^a	Mp (°C)	Mp ^{Ref} (°C)
22		 4v	35	88	216–218	214–216 ³⁶
23		 4w	70	87	184–186	180–182 ²⁹
24		 4x	65	84	187–189	185–188 ³⁹
25		 4y	70	88	204–206	203–205 ³⁴

Reaction conditions: aldehyde **1a–1y** (1 mmol), dimedone **2** (1 mmol), malononitrile **3** (1 mmol), and 11.7 mg of NiFe₂O₄ MNPs (5% mol) in ethanol solvent at 40 °C.

^a: Isolated yield.

2.3. Conclusions

In this study, the application of an inexpensive, ecofriendly, magnetically recoverable, and reusable catalyst provides an efficient and suitable method for the synthesis of substituted 4*H*-chromenes in recent synthetic methodologies. The present procedure has many advantages such as the use of a green solvent and nanocatalyst, operational simplicity, easy workup of products, nonchromatographic purification technique, environmentally benign conditions, short reaction time, and high yields.

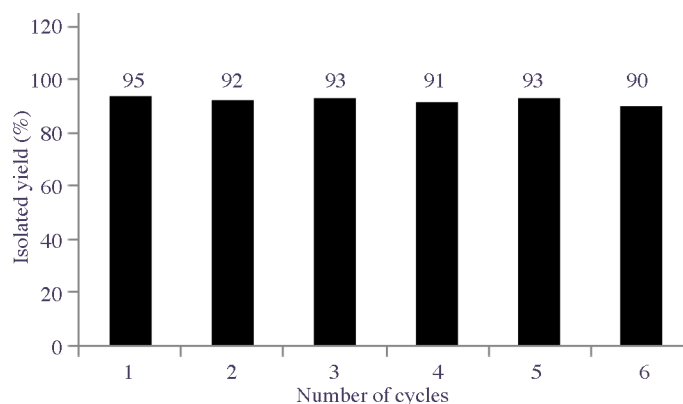


Figure 8. Reusability of NiFe_2O_4 MNPs for the synthesis of compound **4a**.

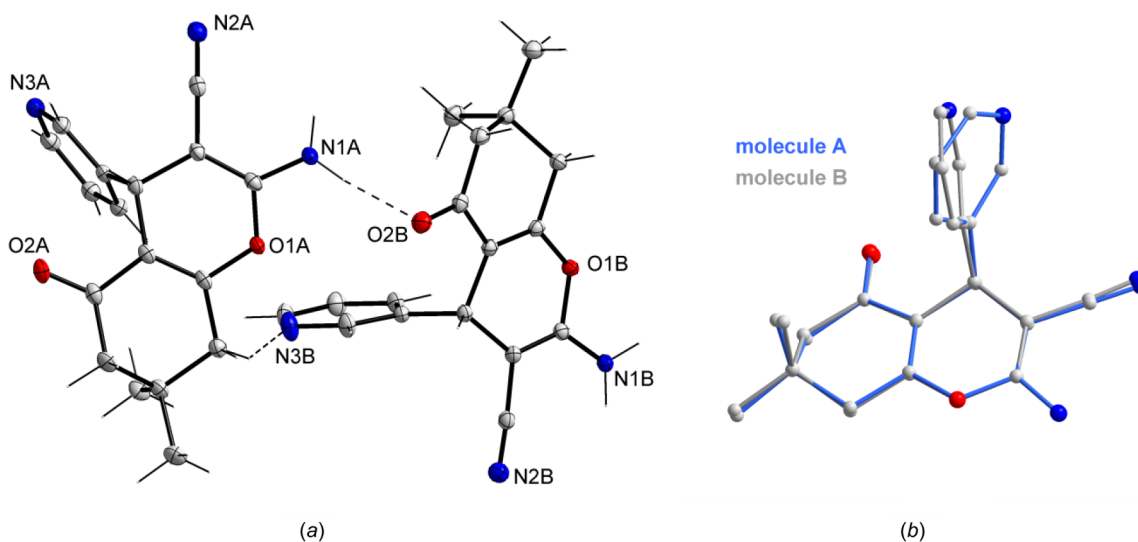


Figure 9. (a) Two crystallographically independent molecules of **4u** present in the asymmetric unit of its crystal, showing the partial atom-numbering scheme and the symmetry-independent hydrogen bonds (dashed lines). The *R* enantiomers are shown (inverted model for molecule **A** has been used). Displacement ellipsoids are drawn at the 50% probability level. (b) Comparison of the conformations of both molecules. H atoms are omitted for clarity. The common reference points are chromene atoms.

3. Experimental

3.1. General comments

All chemical materials were purchased from Sigma-Aldrich (USA), Merck (Germany), Fluka (Switzerland), or Daejung (Korea) and were applied without any further purification. The structure of NiFe_2O_4 MNPs was analyzed by XRD with an X'Pert-PRO advanced diffractometer using $\text{Cu}(\text{K}\alpha)$ radiation (wavelength: 1.5406 Å), operated at 40 kV and 40 mA in the range of 2θ from 20° to 70° at room temperature. The morphology and particle size of the nanoparticles were evaluated by SEM (KYKY Co., Model EM 3200, China). The disk was covered with gold in an ionization chamber. TEM was analyzed using a Zeiss-EM10C TEM instrument with accelerating voltage of 80 kV.

All of the reactions were monitored by TLC with UV light. FT-IR spectrophotometer spectra were

obtained on a Jasco 6300 FT-IR spectrometer. Melting points of products were measured by an Electrothermal 9100 apparatus (Labequip Ltd., Markham, Canada) and are uncorrected. ^1H and ^{13}C NMR (DMSO- d_6) spectra were recorded on a Bruker DRX-250 Avance spectrometer at 250.13 and 62.90 MHz, respectively.

3.2. Procedure for the preparation of NiFe_2O_4 MNPs

NiFe_2O_4 was synthesized via the autocombustion assisted sol-gel method from Fe(III) and Ni(II) ions (molar ratio 2:1) in ammonia solution. In summary, iron(III) nitrate nonahydrate (2 mmol), nickel(II) nitrate hexahydrate (1 mmol), and citric acid as a chelating agent (3 mmol) were dissolved in deionized water. The pH value of the solution was controlled at 7 by adding ammonia solution (25%) dropwise to the reaction mixture under fixed stirring. The solution was heated on a water bath at 60 °C until the formation of a gummy gel and then the temperature was increased to 80 °C to produce a stiff gel. Subsequently, the temperature of the prepared gel was increased to ca. 200 °C for autocombustion. With the exhaust of gases like CO_2 , H_2O , and N_2 a dark brown powder was obtained. The ferrite powder was rinsed with deionized water and acetone several times and separated with a strong external magnet.

3.3. General procedure for the synthesis of substituted 4H-chromenes (4a–4y)

A solution of aldehyde **1a–1y** (1 mmol), dimedone **2** (1 mmol), malononitrile **3** (1 mmol), and ethanol (4 mL) was magnetically stirred at room temperature. To the mixture, NiFe_2O_4 MNPs (5 mol%) were added and the content was heated at 40 °C for the appropriate time. The progress of the reaction was checked by TLC (n-hexane:EtOAc, 10:6). After completion, the resulting product was heated in ethanol. The catalyst was magnetically removed from the mixture and washed several times with ethanol for reuse. The pure product was collected from the filtrate after cooling to room temperature with an ice bath and then was recrystallized from hot ethanol.

3.3.1. Representative procedure for synthesis of 4a

A solution of 4-chlorobenzaldehyde (141 mg, 1 mmol), dimedone (140 mg, 1 mmol), malononitrile (66 mg, 1 mmol), and ethanol (2 mL) was magnetically stirred at room temperature. To the mixture, NiFe_2O_4 MNPs (5 mol%) were added and the content was heated at 40 °C for the appropriate time. The progress of the reaction was checked by TLC (n-hexane:EtOAc, 10:6). After completion, the resulting product was heated in ethanol. The catalyst was magnetically removed from the mixture and washed several times with acetone for reuse. The pure product was collected from the filtrate after cooling to room temperature with an ice bath. The pure product was obtained by recrystallization from hot ethanol.

3.3.2. Spectral data of the selected products

3.3.2.1. 2-Amino-4-(4-chlorophenyl)-7,7-dimethyl-5-oxo-5,6,7,8-tetrahydro-4H-chromene-3-carbonitrile (4a)

White crystal; yield 95%; mp 214–216 °C. IR (KBr): ν_{max} 3390, 3321, 3188, 2940, 2891, 2192, 1683, 1714 cm^{-1} . ^1H NMR (DMSO- d_6 , 250.13 MHz): δ_{H} 0.91 (s, 3H, CH_3), 1.00 (s, 3H, CH_3), 2.34 (d, $J = 16.01$ Hz, 1H, CH_2), 2.07 (d, $J = 16.01$ Hz, 1H, CH_2), 2.23 (s, 2H, CH_2), 4.16 (s, 1H, CH), 7.03 (s, 2H, NH_2), 7.13 (d, $J = 7.00$ Hz, 2H, arom.), 7.33 (d, $J = 7.00$ Hz, 2H, arom.) ppm. ^{13}C NMR (DMSO- d_6 , 62.90 MHz):

δ_C 27.28, 28.76, 31.11, 32.23, 35.56, 50.37, 58.21, 112.78, 120.02, 128.75, 129.58, 131.60, 144.19, 158.95, 163.08, 196.15 ppm.

3.3.2.2. 2-Amino-4-(4-isopropylphenyl)-7,7-dimethyl-5-oxo-5,6,7,8-tetrahydro-4H-chromene-3-carbonitrile (4l)

White solid; yield 89%; mp 206–208 °C. IR (KBr): ν_{\max} 3390, 3325, 3213, 2963, 2872, 2189, 1682, 1603, 1365 cm^{-1} . ^1H NMR (DMSO- d_6 , 250.13 MHz): δ_H 0.95 (s, 3H, CH_3), 1.02 (s, 3H, CH_3), 1.14 (d, 3H, CH_3), 1.17 (d, 3H, CH_3), 2.09 (d, $J = 16.01$ Hz, 1H, CH_2), 2.37 (d, $J = 16.26$ Hz, 1H, CH_2), 2.50 (s, 2H, CH_2), 2.96 (hpt, 1H, $\text{CH}(\text{CH}_3)_2$), 4.12 (s, 1H, CH), 6.94 (s, 2H, NH_2), 7.03 (d, $J = 7.75$ Hz, 2H, arom.), 7.14 (d, $J = 8.00$ Hz, 2H, arom.) ppm. ^{13}C NMR (DMSO- d_6 , 62.90 MHz): δ_C 24.34, 27.36, 28.81, 32.25, 33.44, 35.58, 50.46, 59.00, 113.29, 120.25, 126.69, 127.43, 142.61, 146.95, 158.91, 162.90, 196.12 ppm.

3.3.2.3. 2-Amino-7,7-dimethyl-4-(4-(methylthio)phenyl)-5-oxo-5,6,7,8-tetrahydro-4H-chromene-3-carbonitrile (4p)

White crystal; yield 90%; mp 239–242 °C; IR (KBr): ν_{\max} 3355, 3257, 3188, 2963, 2192, 1683, 1652, 1369 cm^{-1} . ^1H NMR (DMSO- d_6 , 250.13 MHz): δ_H 0.94 (s, 3H, CH_3), 1.01 (s, 3H, CH_3), 2.08 (d, $J = 15.25$ Hz, 1H, CH_2), 2.23 (d, $J = 14.26$ Hz, 1H, CH_2), 2.42 (s, 2H, CH_2), 2.48 (s, 3H, SCH_3), 4.14 (s, 1H, CH), 6.98 (s, 2H, NH_2), 7.15 (d, $J = 7.25$ Hz, 2H, arom.), 7.09 (d, $J = 7.00$ Hz, 2H, arom.) ppm. ^{13}C NMR (DMSO- d_6 , 62.90 MHz): δ_C 15.19, 27.27, 28.84, 32.22, 35.58, 50.44, 58.66, 113.09, 120.13, 126.43, 128.29, 136.55, 141.98, 144.19, 158.91, 162.84, 196.08 ppm.

3.3.2.4. 2-Amino-7,7-dimethyl-4-(5-nitrofuran-2-yl)-5-oxo-5,6,7,8-tetrahydro-4H-chromene-3-carbonitrile (4r)

Yield 83%; pale yellow solid; mp 180–183 °C. IR (KBr): ν_{\max} 3406, 3335, 3221, 2964, 2199, 1686, 1490, 1350 cm^{-1} . ^1H NMR (DMSO- d_6 , 250.13 MHz): δ_H 1.00 (s, 3H, CH_3), 1.04 (s, 3H, CH_3), 2.17 (d, $J = 16.01$ Hz, 1H, CH_2), 2.32 (d, $J = 16.01$ Hz, 1H, CH_2), 2.46 (d, $J = 17.51$ Hz, 1H, CH_2), 2.58 (d, $J = 17.51$ Hz, 1H, CH_2), 4.51 (s, 1H, CH), 6.63 (d, $J = 6.5$ Hz, 1H, arom.), 7.31 (s, NH_2), 7.61 (1H, d, $J = 6.75$ Hz, 2H, arom.) ppm. ^{13}C NMR (DMSO- d_6 , 62.90 MHz): δ_C 26.75, 28.87, 30.28, 32.33, 50.17, 54.02, 109.02, 110.52, 114.92, 119.33, 150.92, 159.65, 160.62, 164.56, 196.04, 3406, 3335, 3221, 2964, 2199, 1686, 1490, 1350 ppm.

3.3.2.5. 2-Amino-7,7-dimethyl-5-oxo-4-(pyridin-3-yl)-5,6,7,8-tetrahydro-4H-chromene-3-carbonitrile (4u)

Yield 85%; white crystal; 223–225 °C; IR (KBr): ν_{\max} 3315, 3181, 2961, 2184, 1682, 1652, 1373 cm^{-1} . ^1H NMR (DMSO- d_6 , 250.13 MHz): δ 0.93 (s, 3H, CH_3), 1.02 (s, 3H, CH_3), 2.10 (d, $J = 16.01$ Hz, 1H, CH_2), 2.24 (d, $J = 16.26$ Hz, 1H, CH_2), 2.54 (s, 2H, CH_2), 4.23 (s, 1H, CH), 7.09 (s, 2H, NH_2), 7.31 (d, $J = 7.75$ Hz, 1H, arom.), 7.52 (d, $J = 7.75$ Hz, 1H, arom.), 8.38 (d, 2H, arom.) ppm. ^{13}C NMR (DMSO- d_6 , 62.90 MHz): δ_C 27.37, 28.66, 32.27, 33.84, 40.12, 50.36, 57.80, 112.26, 119.91, 124.08, 135.17, 128.75, 140.46, 148.29, 149.13, 159.04, 163.40, 196.16 ppm.

3.3.3. X-ray crystallography

After recrystallization of compound **4u**, the pure solid was dissolved in hot ethanol. By X-ray, proper crystals of **4u** appeared after slow evaporation of its solvent at room temperature.

The crystallographic measurement of **4u** was performed on an Xcalibur R κ -geometry automated four-circle diffractometer equipped with a Ruby CCD camera and graphite-monochromated Mo K α radiation ($\lambda = 0.71073 \text{ \AA}$). The data were collected at 80(2) K using an Oxford Cryosystems cooler. Data were corrected for Lorentz and polarization effects. Data collection, cell refinement, data reduction and analysis, and empirical absorption correction were carried out with Xcalibur R software and CrysAlisPro.⁴¹ The structure was solved by direct methods with SHELXS97⁴² and refined by a full-matrix least-squares technique with SHELXL2016⁴³ with anisotropic thermal parameters for non-H atoms. All H atoms were found in different Fourier maps and were refined isotopically. In the final refinement cycles, the C-bonded H atoms were repositioned in their calculated positions and refined using a riding model, with C–H = 0.95–1.00 \AA and with $U_{iso}(\text{H}) = 1.2U_{eq}(\text{C})$ for CH and CH₂ or $1.5U_{eq}(\text{C})$ for CH₃. Amine H atoms were refined freely. The figure was made with the DIAMOND program.⁴⁴ The crystallographic information file (CIF) was deposited with the Cambridge Crystallographic Data Centre (<http://www.ccdc.cam.ac.uk/>; deposition number CCDC 1511770) and provided as ESI.

Crystal data for 4u: C₁₇H₁₇N₃O₂, $M_r = 341.33$, colorless block, crystal size $0.48 \times 0.32 \times 0.13$ mm, triclinic, space group $P\bar{1}$ (No. 2), $a = 8.623(2)$, $b = 13.632(4)$, $c = 14.824(4) \text{ \AA}$, $\alpha = 114.65(3)^\circ$, $\beta = 94.60(3)^\circ$, $\gamma = 99.80(3)^\circ$, $V = 1538.2(8) \text{ \AA}^3$, $T = 80(2) \text{ K}$, $Z = 4$, $\mu = 0.09 \text{ mm}^{-1}$, 12,458 reflections measured, 8255 unique ($R_{int} = 0.020$), 6420 observed ($I > 2\sigma(I)$), $(\sin \theta/\lambda)_{max} = 0.720 \text{ \AA}^{-1}$, 413 parameters, 0 restraints, $R = 0.047$, $wR = 0.103$ (observed refl.), $GOOF = S = 1.03$, $(\Delta\rho_{max}) = 0.38$ and $(\Delta\rho_{min}) = -0.24 \text{ e \AA}^{-3}$.

Acknowledgment

This work was funded by grant NRF-2015-002423 of the National Research Foundation of Korea.

References

1. Tarannum, S.; Siddiqui, Z. N. *Monatsh. Chem.* **2017**, *148*, 717-730.
2. Ahankar, H.; Ramazani, A.; Ślepokura, K.; Lis, T.; Joo, S. W. *Green Chem.* **2016**, *18*, 3582-3593.
3. Shajari, N.; Kazemizadeh, A. R.; Ramazani, A. *Turk. J. Chem.* **2015**, *39*, 874-879.
4. Ramazani, A.; Dastanra, K.; Nasrabadi, F. Z.; Karimi, Z.; Rouhani, M.; Hosseini, M. *Turk. J. Chem.* **2012**, *36*, 467-476.
5. Mobinikhaledi, A.; Yazdanipour, A.; Ghashang, M. *Turk. J. Chem.* **2015**, *39*, 667-675.
6. Karami, B.; Eskandari, K.; Ghasemi, A. *Turk. J. Chem.* **2012**, *36*, 601-613.
7. Taghavi Fardood, S.; Ramazani, A.; Moradi, S. *J. Sol-Gel Sci. Technol.* **2017**, *82*, 432-439.
8. Shouli, A.; Menati, S.; Sayyahi, S. *C. R. Chimie* **2017**, *20*, 765-772.
9. Ghahremanzadeh, R.; Rashid, Z.; Zarnani, A. H.; Naeimi, H. *Appl. Catal. A* **2013**, *467*, 270-278.
10. Senapati, K. K.; Borgohain, C.; Phukan, P. *J. Mol. Catal. A Chem.* **2011**, *339*, 24-31.
11. Ahankar, H.; Ramazani, A.; Joo, S. W. *Res. Chem. Intermed.* **2016**, *42*, 2487-2500.
12. Li, P.; Li, Z.; Zhai, F.; Wan, Q.; Li, X.; Qu, X.; Volinsky, A. A. *J. Phys. Chem. C* **2013**, *117*, 25917-25925.

13. Ellis, G. P. *Chromenes, Chromanones, and Chromones: Chemistry of Heterocyclic Compounds Chromenes, Vol. 31*. Wiley: New York, NY, USA, 1977.
14. Reboul, E.; Richelle, M.; Perrot, E.; Desmoulins-Malezet, C.; Pirisi, V.; Borel, P. *J. Agric. Food Chem.* **2006**, *54*, 8749-8755.
15. Kudoh, S.; Okada, H.; Nakahira, K.; Nakamura, H. *Anal. Sci.* **1990**, *6*, 53-56.
16. Hufford, C. D.; Oguntimein, B. O.; Van Engen, D.; Muthard, D.; Clardy, J. *J. Am. Chem. Soc.* **1980**, *102*, 7365-7367.
17. Wandji, J.; Fomum, Z. T.; Tillequin, F.; Libot, F.; Koch, M. *J. Nat. Prod.* **1995**, *58*, 105-108.
18. van Otterlo, W. A.; Ngidi, E. L.; Kuzvidza, S.; Morgans, G. L.; Moleele, S. S.; de Koning, C. B. *Tetrahedron* **2005**, *61*, 9996-10006.
19. Victorine, F.; Augustin, E. *J. Nat. Prod.* **1998**, *61*, 380-383.
20. Mohr, S. J.; Chirigos, M. A.; Fuhrman, F. S.; Pryor, J. W. *Cancer Res.* **1975**, *35*, 3750-3754.
21. Flavin, M. T.; Rizzo, J. D.; Khilevich, A.; Kucherenko, A.; Sheinkman, A. K.; Vilaychack, V.; Lin, L.; Chen, W.; Greenwood, E. M.; Pengsuparp, T. *J. Med. Chem.* **1996**, *39*, 1303-1313.
22. Moon, D. O.; Kim, K. C.; Jin, C. Y.; Han, M. H.; Park, C.; Lee, K. J.; Park, Y. M.; Choi, Y. H.; Kim, G. Y. *Int. Immunopharmacol.* **2007**, *7*, 222-229.
23. Raj, T.; Bhatia, R. K.; Sharma, M.; Saxena, A.; Ishar, M. *Eur. J. Med. Chem.* **2010**, *45*, 790-794.
24. Manolov, I.; Maichle-Moessmer, C.; Danchev, N. *Eur. J. Med. Chem.* **2006**, *41*, 882-890.
25. Sharma, U.; Sharma, U.; Singh, A.; Agarwal, V. *J. Pharmacol. Res.* **2010**, *1*, 17-20.
26. Zhang, Y. L.; Chen, B. Z.; Zheng, K. Q.; Xu, M. L.; Lei, X. H.; Yaoxue, X. B. *Chem. Abstr.* **1982**, *96*, 135383e.
27. Hafez, E. A. A.; Elnagdi, M. H.; Elagamey, A. G. A.; El-Taweel, F. M. A. A. *Heterocycles* **1987**, *26*, 903-907.
28. Safaei, H. R.; Shekouhy, M.; Shirinfeshan, A.; Rahmanpur, S. *Mol. Divers.* **2012**, *16*, 669-683.
29. Pandit, K. S.; Chavan, P. V.; Desai, U. V.; Kulkarni, M. A.; Wadgaonkar, P. P. *New J. Chem.* **2015**, *39*, 4452-4463.
30. Fang, D.; Zhang, H. B.; Liu, Z. L. *J. Heterocycl. Chem.* **2010**, *47*, 63-67.
31. Sun, W. B.; Zhang, P.; Fan, J.; Chen, S. H.; Zhang, Z. H. *Synth. Commun.* **2010**, *40*, 587-594.
32. Gao, S.; Tsai, C. H.; Tseng, C.; Yao, C. F. *Tetrahedron* **2008**, *64*, 9143-9149.
33. Gurusurthi, S.; Sundari, V.; Valliappan, R. *J. Chem.* **2009**, *6*, S466-S472.
34. Dekamin, M. G.; Eslami, M.; Maleki, A. *Tetrahedron* **2013**, *69*, 1074-1085.
35. Shirini, F.; Daneshvar, N. *RSC Adv.* **2016**, *6*, 110190-110205.
36. Sharma, N.; Banerjee, B.; Brahmachari, G.; Kant, R.; Gupta, V. *Crystallogr. Rep.* **2015**, *60*, 1126-1130.
37. Naimi-Jamal, M. R.; Mashkouri, S.; Sharifi, A. *Mol. Divers.* **2010**, *14*, 473-477.
38. Khoobi, M.; Ma'mani, L.; Rezazadeh, F.; Zareie, Z.; Foroumadi, A.; Ramazani, A.; Shafiee, A. *J. Mol. Catal. A Chem.* **2012**, *359*, 74-80.
39. Rajput, J. K.; Kaur, G. *Catal. Sci. Technol.* **2014**, *4*, 142-151.
40. Safari, J.; Javadian, L. *Ultrason. Sonochem.* **2015**, *22*, 341-348.
41. Oxford Diffraction Ltd. *CrysAlisCCD and CrysAlisRED in KM4-CCD Software*. Oxford Diffraction Ltd.: Abingdon, UK, 2010.
42. Sheldrick, G. M. *Acta Crystallogr. A* **2008**, *64*, 112-122.
43. Sheldrick, G. M. *Acta Crystallogr. C* **2015**, *71*, 3-8.
44. Brandenburg, K. *DIAMOND Version 3.2k*. Crystal Impact GbR: Bonn, Germany, 2014.